HAL
open science

A new empirical model for radar scattering from bare soil surfaces

Nicolas Baghdadi, M. Choker, Mehrez Zribi, Mohammad El Hajj, S. Paloscia, N.E.C. Verhoest, H. Lievens, Frédéric Baup, F. Mattia

To cite this version:

Nicolas Baghdadi, M. Choker, Mehrez Zribi, Mohammad El Hajj, S. Paloscia, et al.. A new empirical model for radar scattering from bare soil surfaces. Reviews on Advanced Materials Science, 2016, 8 (11), pp.920. 10.3390/rs8110920 . hal-01529350

HAL Id: hal-01529350

https://hal.science/hal-01529350v1

Submitted on 30 May 2017

HAL is a multi-disciplinary open access archive for the deposit and dissemination of scientific research documents, whether they are published or not. The documents may come from teaching and research institutions in France or abroad, or from public or private research centers.

L'archive ouverte pluridisciplinaire **HAL**, est destinée au dépôt et à la diffusion de documents scientifiques de niveau recherche, publiés ou non, émanant des établissements d'enseignement et de recherche français ou étrangers, des laboratoires publics ou privés.

remote sensing

MDPI

Article

A New Empirical Model for Radar Scattering from Bare Soil Surfaces

Nicolas Baghdadi[1], Mohammad Choker[1], Mehrez Zribi[2], Mohammad El Hajj[1], Simonetta Paloscia[3], Niko E.C. Verhoest[4], Hans Lievens[4,5], Frederic Baup[2], Francesco Mattia[6]

[1] IRSTEA, UMR TETIS, 500 rue François Breton, F-34093 Montpellier cedex 5, France ;
E-Mails : nicolas.baghdadi@teledetection.fr; mohammad.choker@teledetection.fr; mohammad.el-hajj@teledetection.fr
[2] CESBIO, 18 av. Edouard Belin, bpi 2801, 31401Toulouse cedex 9, France;
E-Mails: mehrez.zribi@ird.fr; frederic.baup@cesbio.cnes.fr
[3] CNR-IFAC, via Madonna del Piano 10, 50019 Sesto Fiorentino, Firenze, Italy;
E-Mail: s.paloscia@ifac.cnr.it
[4] Laboratory of Hydrology and Water Management, Ghent University, Ghent B-9000, Belgium;
E-Mails: niko.verhoest@UGent.be ; hans.lievens@UGent.be
[5] Global Modeling and Assimilation Office, NASA Goddard Space Flight Center, Greenbelt, MD 20771 USA;
E-Mails: Hans.Lievens@UGent.be (H.L.)
[6] CNR-ISSIA, via Amendola 122/D, Bari 70126, Italy; E-Mail: mattia@ba.issia.cnr.it

Abstract: The objective of this paper is to propose a new semi-empirical radar backscattering model for bare soil surfaces based on the Dubois model. A wide dataset of backscattering coefficients extracted from SAR (synthetic aperture radar) images and in situ soil surface parameter measurements (moisture content and roughness) is used. The retrieval of soil parameters from SAR images remains challenging because the available backscattering models have limited performances. Existing models, physical, semi-empirical or empirical, do not allow for a reliable estimate of soil surface geophysical parameters for all surface conditions. The proposed model, developed in HH, HV and VV polarizations, uses a formulation of radar signals based on physical principles that validated in numerous studies. Never before has a backscattering model been built and validated on such an important dataset as the one proposed in this study. It contains a wide range of incidence angles (18°-57°) and radar wavelengths (L, C, X), well distributed geographically for regions with different climate conditions (humid, semi-arid and arid sites) and involving many SAR sensors.The results show that the new model shows a very good performance for different radar wavelength (L, C, X), incidence angles, and polarizations (RMSE about 2 dB). This model is easy to invert and could provide a way to improve the retrieval of soil parameters.

Keywords: New backscattering model, Dubois model, SAR images, Soil parameters.

1. Introduction

Soil moisture content and surface roughness play an important roles in meteorology, hydrology, agronomy, agriculture, and risk assessment. These soil surface characteristics can be estimated using synthetic aperture radar (SAR). Today, several high-resolution SAR images can be acquired on a given study site with the availability of SAR data in L-band (ALOS-2), C-band (Sentinel-1), and X-band (TerraSAR-X, COSMO-SkyMed). In addition, it is possible to obtain SAR and optical data for global areas at high spatial and temporal resolutions with free and open access Sentinel-1/2 satellites (6 days with the two Sentinel-1 and 5 days with the two Sentinel-2 satellites at 10 m spatial resolution). This availability of both Sentinel-1 satellites and Sentinel-2 sensors in addition to Landsat-8 (also free and open access) allows the combination of SAR and optical data to estimate soil moisture and vegetation parameters in operational mode.

The retrieval of soil moisture content and surface roughness requires the use of radar backscatter models capable of correctly modeling the radar signal for a wide range of soil parameter values. This estimation from imaging radar data implies the use of backscattering electromagnetic models, which can be physical, semi-empirical or empirical. The physical models (e.g., Integral Equation Model "IEM," Small Perturbation Model "SPM," Geometrical Optic Model "GOM," Physical Optic Model "POM," etc.) based on physical approximations corresponding to a range of surface conditions (moisture and roughness) provide site-independent relationships but have limited validity depending upon the soil roughness. As for semi-empirical or empirical models, they are often difficult to apply to sites other than those on which they were developed and are generally valid only for specific soil conditions. The empirical models are often favored by users because the models are easier to implement and invert [1–7].

Among the numerous semi-empirical models reported in the literature, the most popular are those developed over bare soils by Oh et al. [8–11] and Dubois et al. [12]. The Oh model uses the ratios of the measured backscatter coefficients HH/VV and HV/VV to estimate volumetric soil moisture (*mv*) and surface roughness (*Hrms*), while the Dubois model links the backscatter coefficients in HH and VV polarizations to the soil's dielectric constant and surface roughness. Extensive studies evaluated various semi-empirical models, but mixed results have been obtained. Some studies show good agreement between measured backscatter coefficients and those predicted by the models, while others have found great discrepancies between them (e.g., [13–16]). The discrepancy between simulations and measurements often reaches several decibels, making soil parameter estimates unusefull.

The objective of this paper is to propose a robust, empirical, radar backscattering model based on the Dubois model. First, the performance of the Dubois model is analyzed using a large dataset acquired at several worldwide study sites by numerous SAR sensors. The dataset consists of SAR data (multi-angular and multi-frequency) and measurements of soil moisture and surface roughness over bare soils. Then, the different terms of Dubois equations that describe the dependence between the SAR signal and both sensor and soil parameters have been validated or modified to improve the modelling of the radar signal. Ultimately, a new semi-empirical backscattering model has been developed for radar scattering in the HH, VV, and HV polarization from bare soil surfaces.

After a description of the dataset in section 2, section 3 describes and analyzes the potential and the limitations of the Dubois model in radar signal simulations over bare soils. In section 4, the new model is described and its performance is evaluated for different available SAR data (L-, C- and X-bands, incidence angles between 20° and 45°). Conclusions are presented in section 5.

2. Dataset description

A wide experimental dataset was used, consisting of SAR images and ground measurements of soil moisture content and roughness collected over bare soils at several agricultural study sites (Table 1). SAR images were acquired by various airborne and spaceborne sensors (AIRSAR, SIR-C, JERS-1, PALSAR-1, ESAR, ERS, RADARSAT, ASAR, TerraSAR-X). The radar data were available in L-, C- and X-bands (approximately 1.25 GHz, 5.3 GHz and 9.6 GHz, respectively); with incidence angles between 18° and 57°; and in HH, VV and HV polarizations. For several reference plots, the mean backscatter coefficients have been obtained from radiometrically and geometrically calibrated SAR images by averaging backscatter coefficient values for each plot for all pixels within the plot.

Table 1. Description of the dataset used in this study. "Fr": France, "It": Italy, "Ge": Germany, "Be": Belgium, "Lu": Luxembourg, "Ca": Canada, "Tu": Tunisia.

Site	SAR sensor	Freq	Year	Number of data
Orgeval (Fr) [17]	SIR-C	L	1994	➢ **HH : 1569 measurements** – **144 in L-band** – **997 in C-band** – **428 in X-band** ➢ **VV : 930 measurements** – **71 in L-band** – **640 in C-band** – **219 in X-band** ➢ **HV : 605 measurements** – **7 in L-band** – **538 in C-band** – **60 in X-band**
Orgeval (Fr) [17–19]	SIR-C, ERS, ASAR	C	1994; 1995; 2008; 2009; 2010	
Orgeval (Fr) [19]	PALSAR-1	L	2009	
Orgeval (Fr) [20]	TerraSAR-X	X	2008, 2009, 2010	
Pays de Caux (Fr) [21–22]	ERS; RADARSAT	C	1998; 1999	
Villamblain (Fr) [23–25]	ASAR	C	2003; 2004; 2006	
Villamblain (Fr) [19,26]	TerraSAR-X	X	2008; 2009	
Thau (Fr) [27]	RADARSAT	C	2010; 2011	
	TerraSAR-X	X	2010	
Touch (Fr) [23,28]	ERS-2; ASAR	C	2004; 2006; 2007	
Mauzac (Fr) [26]	TerraSAR-X	X	2009	
Garons (Fr) [26]	TerraSAR-X	X	2009	
Kairouan (Tu) [29]	ASAR	C	2012	
Kairouan (Tu) [26,29, 30]	TerraSAR-X	X	2010; 2012; 2013; 2014	
Yzerons (Fr) [31]	TerraSAR-X	X	2009	
Versailles (Fr) [26]	TerraSAR-X	X	2010	
Seysses (Fr) [26]	TerraSAR-X	X	2010	
Chateauguay (Ca) [21]	RADARSAT	C	1999	
Brochet (Ca) [21]	RADARSAT	C	1999	
Alpilles (Fr) [21]	ERS; RADARSAT	C	1996; 1997	
Sardaigne (It) [32]	ASAR; RADARSAT	C	2008; 2009	
Saint Lys (Fr) [33]	PALSAR-1	L	2010	
Matera (It) [34]	SIR-C	L	1994	
Alzette (Lu) [35]	PALSAR-1	L	2008	
Dijle (Be) [35]	PALSAR-1	L	2008; 2009	
Zwalm (Be) [35]	PALSAR-1	L	2007	
Demmin (Ge) [35]	ESAR	L	2006	
Montespertoli (It) [36]	AIRSAR	L	1991	
Montespertoli (It) [37]	SIR-C	L; C	1994	
Montespertoli (It) [38]	JERS-1	L	1994	

In addition, in situ measurements of soil moisture (*mv*) were available for each reference plot. The soil water content was collected from the top 5 or 10 cm of each reference plot at several locations using the gravimetric method and a calibrated TDR (time domain reflectometry) probe. In practice, the soil moisture for each reference plot was assumed to be equal to the mean of all measurements carried out on the reference plot within a few hours of the SAR overpasses. In our experimental dataset, the soil moisture ranged from 2 to 47 vol.%.

The roughness was defined by the standard deviation of surface height (*Hrms*) available for each reference plot. From roughness profiles sampled for each reference plot using mainly laser or needle profilometers (mainly 1 m and 2 m long and with 1 cm and 2 cm sampling intervals), the mean of all experimental autocorrelation functions was calculated to estimate the *Hrms* measurement. However, for some in situ measurement campaigns, meshboard technique was used for estimating the roughness parameters. In our dataset, *Hrms* surface height ranged from 0.2 to 9.6 cm (*k Hrms* ranged from 0.2 and 13.4, *k* was the radar wave number).

A total of 1569 experimental data acquisitions with radar signal, soil moisture content and roughness were available for HH polarization, 930 for VV polarization, and 605 for HV polarization.

3. Validation and analysis of the Dubois model

3.1. Description of the Dubois model

Dubois et al. [12] proposed an empirical model to model radar backscatter coefficients in HH and VV polarizations (σ^0_{HH} and σ^0_{VV}) for bare soil surfaces. The expressions of σ^0_{HH} and σ^0_{VV} depend on the radar wave incidence angle (θ, in radians), the real part of the soil dielectric constant (ε), the rms surface height of the soil (*Hrms*), the radar wavelength (λ=2π/*k*, where *k* is the radar wavenumber):

$$\sigma^0_{HH} = 10^{-2.75}\left(\frac{\cos^{1.5}\theta}{\sin^5\theta}\right)10^{0.028\varepsilon\tan\theta}\left(k\,Hrms\sin\theta\right)^{1.4}\lambda^{0.7} \quad (1)$$

$$\sigma^0_{VV} = 10^{-2.35}\left(\frac{\cos^{3}\theta}{\sin^3\theta}\right)10^{0.046\varepsilon\tan\theta}\left(k\,Hrms\sin\theta\right)^{1.1}\lambda^{0.7} \quad (2)$$

σ^0_{HH} and σ^0_{VV} are given in a linear scale. λ is in cm. The validity of the Dubois model is defined as follows: $k\,Hrms \leq 2.5$, $mv \leq 35$ vol. %, and $\theta \geq 30°$.

3.2. Comparison between simulated and real data

The Dubois model shows an overestimation of the radar signal by 0.7 dB in HH polarization and an underestimation of the radar signal by 0.9 dB in VV polarization for all data combined (Table 2). The results show that the overestimation in HH is of the same order for L-, C- and X-bands (between 0.6 dB and 0.8 dB). For the L-band, a slight overestimation of approximately 0.2 dB of SAR data is observed in VV polarization. Also in VV polarization, Dubois model based simulations underestimate the SAR data in C- and X-bands by approximately 0.7 dB and 2.0 dB, respectively.

The rms error (RMSE) is approximately 3.8 dB and 2.8 dB in HH and VV, respectively (Table 2). Analysis of the RMSE according the radar frequency band (L, C and X separately) shows in HH an increase of the RMSE with the radar frequency (2.9 dB in L-band, 3.7 dB in C-band, and 4.1 dB in X-band). In VV polarization, the quality of Dubois simulations (RMSE) is similar for L- and C-bands but is less accurate in X-band (2.3 dB in L-band, 2.6 dB in C-band, and 3.2 dB in X-band).

Table 2. Comparison between the Dubois model and real data for all data and by range of *kHrms*, soil moisture (*mv*) and incidence angle (θ). Bias = real data – model.

	Dubois for HH		**Dubois for VV**	
	Bias (dB)	**RMSE (dB)**	**Bias (dB)**	**RMSE (dB)**
For all data	-0.7	3.8	+0.9	2.8
L-band	-0.8	2.9	-0.2	2.3
C-band	-0.6	3.7	+0.7	2.6
X-band	-0.7	4.1	+2.0	3.2
kHrms < 2.5	+0.4	3.4	+1.3	2.9
kHrms > 2.5	-2.7	4.5	-0.1	2.5
mv < 20 vol.%	-2.0	4.3	+0.9	2.8
mv > 20 vol. %	+0.5	3.2	+0.9	2.8
$\theta < 30°$	-4.1	5.4	-0.6	2.9
$\theta > 30°$	+0.6	3.0	+1.5	2.7

In addition, the agreement between Dubois model simulations and SAR data is analyzed according to soil roughness, moisture content and incidence angle (Figures 1 and 2). The results indicate a slight underestimation of the radar signal by the Dubois model in the case of *kHrms* lower than 2.5 (Dubois validation domain) for both HH and VV polarizations (Figures 1b, 2b; Table 2). For surfaces with a roughness *kHrms* greater than 2.5, an overestimation of the radar signal is obtained with the Dubois model in HH while the model works correctly in VV (Figures 1b, 2b; Table 2). Higher under- and overestimations are observed in HH than they are in VV (reach approximately 10 dB in HH).

Analysis of the error as a function of soil moisture (*mv*) shows that for both VV-polarized data, whatever the *mv*-values, and HH-polarized data with *mv*-values higher than 20 vol.%, the observed bias between real and simulated data is small (Figures 1c, 2c; Table 2). However, a strong overestimation of the radar signal is observed by the Dubois model in HH for *mv*-values lower than 20 vol.% (-2.0 dB, Table 2).

Finally, the discrepancy between SAR and the model is larger in HH for incidence angles lower than 30° (outside of the Dubois validity domain) than for incidence angles higher than 30° (Table 2). The Dubois model strongly overestimates the radar signal in HH for incidence angles lower than 30° but agrees closely with the measured data for incidence angles higher than 30° (Figures 1d, 2d; Table 2). In VV polarization, the Dubois model slightly overestimates the radar signal for incidence angles lower than 30° and underestimates the signal for incidence angles higher than 30° by +1.5 dB (Figures 1d, 2d; Table 2).

In conclusion, the Dubois model simulates VV better than it does HH (RMSE=2.8 and 3.8 dB, respectively). The disagreements observed between the Dubois model and measured data are not limited to data that are outside the optimal application domain of the Dubois model.

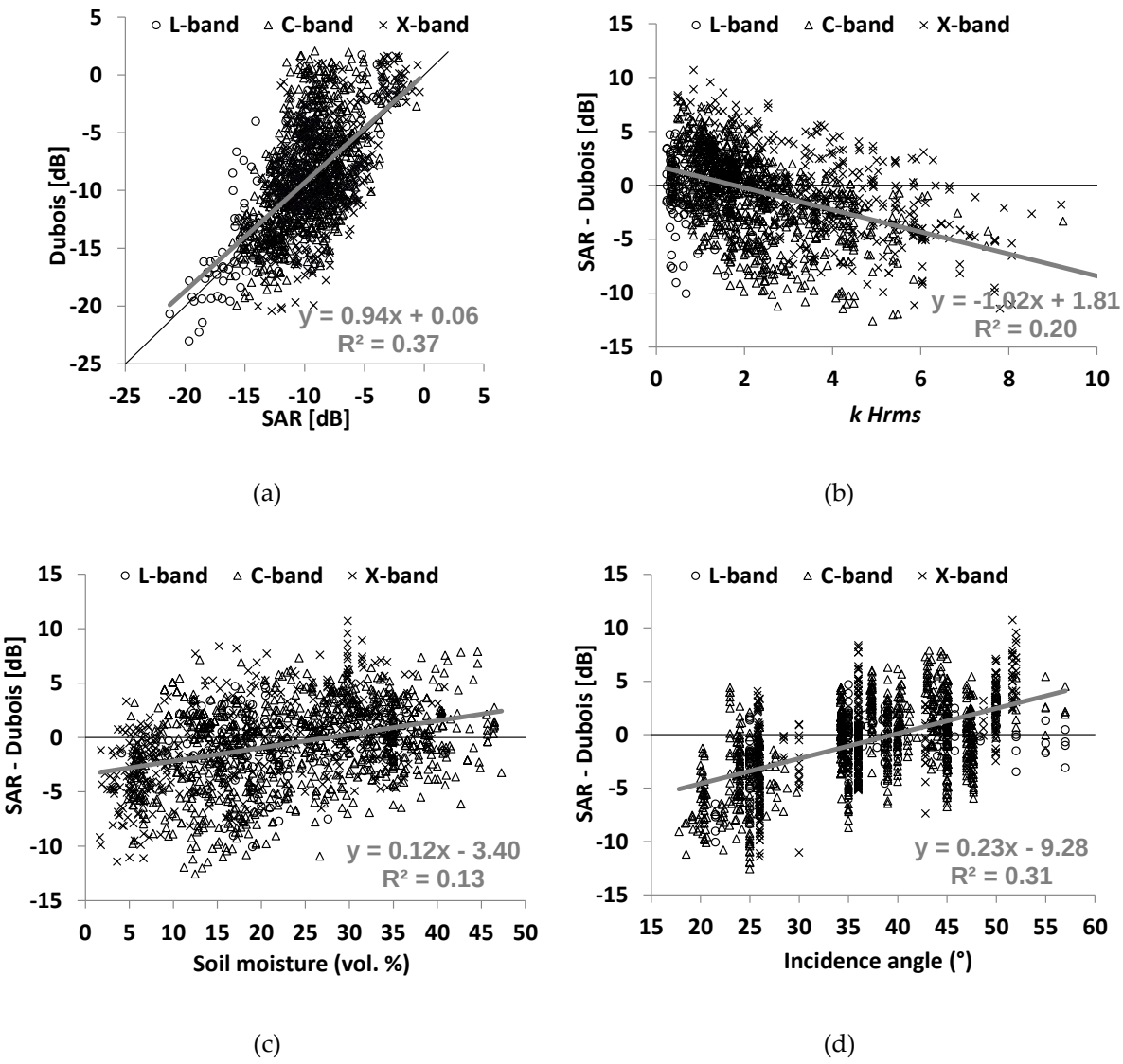

Figure 1. For HH polarization, (a) comparison between radar backscattering coefficients calculated from SAR images and estimated from the Dubois model, (b) difference between the SAR signal and the Dubois model relative to soil roughness (*kHrms*), (c) difference between the SAR signal and the Dubois model relative to soil moisture (*mv*), (d) difference between the SAR signal and the Dubois model relative to incidence angle. The best regression model is ploted in gray.

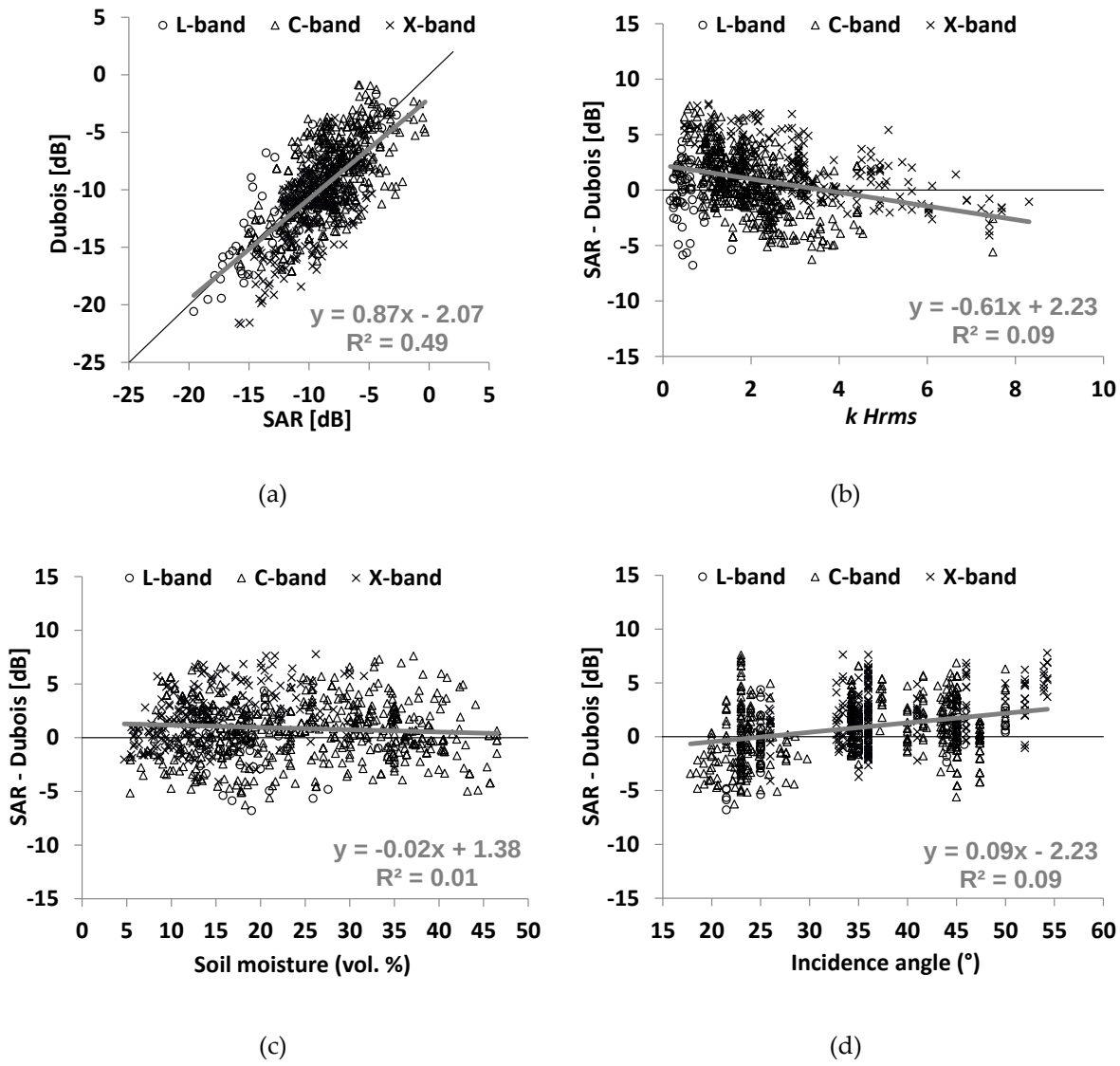

Figure 2. For VV polarization, (a) comparison between radar backscattering coefficients calculated from SAR images and estimated from the Dubois model, (b) difference between the SAR signal and the Dubois model relative to soil roughness (*kHrms*), (c) difference between the SAR signal and the Dubois model relative to soil moisture (*mv*), (d) difference between the SAR signal and the Dubois model relative to incidence angle. The best regression model is ploted in gray.

4. New empirical model

4.1. Methodology

The disagreement observed between measured and modelled radar signal encouraged us to develop a new empirical backscattering model using SAR observations and soil in situ measurements. The new model is based on the Dubois model and uses the dependency observed between the SAR signal and soil parameters according to results obtained in various studies. For bare soils, the backscattering coefficient depends on soil parameters (roughness and moisture) and SAR instrumental parameters (incidence angle, polarization and wavelength). For bare soils, the radar signal in pq polarization (p and q = H or V, with HV=VH) can be expressed as the product of three components:

$$\sigma_{pq}^{\circ} = f_{pq}(\theta)\, g_{pq}(mv,\theta)\ \Gamma_{pq}(kHrms,\theta) \tag{3}$$

The radar backscatter coefficient is related to the incidence angle (θ) by the relation $f_{pq}(\theta) = \alpha(\cos\theta)^{\beta}$ ([39-41]). This relationship describes the decrease of σ° with the incidence angle (decrease higher for low angles than for high angles).

The second term represents the relationship between the radar backscatter coefficient and soil moisture (*mv)*. The results obtained in several investigations show that, for bare soils, the radar signal (σ°) in decibels increases linearly with soil moisture (*mv*) when *mv* is in the range between approximately 5 and 35 vol.% (e.g., [5,6,19,42]). In linear scale $g_{pq}(mv,\theta)$ can be written as $\delta\, 10^{\gamma\, mv}$. The sensitivity of the radar signal to the soil moisture γ depends on θ. Higher sensitivity is observed for low than for high incidence angles (e.g., [43,44]). To include this dependence on incidence angle, the soil moisture value is multiplied with the term $cotan(\theta)$. Thus, $g_{pq}(mv,\theta)$ can be written as $\delta\, 10^{\gamma\, cotan(\theta)\, mv}$.

The last term $\Gamma_{pq}(kHrms,\theta)$ represents the behaviour of σ° with soil roughness. An exponential or logarithmic function is often used to express the radar signal (in dB) in terms of surface roughness ([7,42,45-46]). For a logarithmic behaviour of σ°(dB) with *k Hrms*, Γ_{pq} in linear scale can be written as $\mu(kHrms)^{\xi}$. Baghdadi et al. [22] showed that at high incidence angles, radar return is highly sensitive to surface roughness and shows much larger dynamics than at a low incidence angle. In addition, the term $sin(\theta)$ is intended to include this dependence with the incidence angle: $\Gamma_{pq=}\mu(kHrms)^{\xi\, sin(\theta)}$.

Finally, the relationship between the radar backscattering coefficient (*σ°*) and the soil parameters (soil moisture and surface roughness) for bare soil surfaces can be written by equation (4):

$$\sigma_{pq}^{\circ} = \delta(\cos\theta)^{\beta}\ 10^{\gamma\, cotan(\theta)\, mv}\ (kHrms)^{\xi\, sin(\theta)} \tag{4}$$

The coefficients δ, β, γ, and ξ are then estimated for each radar polarization using the method of least squares by minimizing the sum of squares of the differences between the measured and modelled radar signal. The error in the modelling of radar backscatter coefficients by the new backscattering model was assessed for each polarization using a 5-fold cross-validation to validate the predictive performance of the new model. To do the 5-fold cross-validation, the dataset was first randomly divided into 5 equal size subsets. Next, 4 of the subsets are used to train the new model and one was retained to validate its predictive performance. The cross-validation process was then repeated 5 times, with each of the 5 sub-datasets used exactly once as the validation data. The final validation result combines the 5 validation results. The advantage of this method over repeated random sub-sampling is that all observations are used for both training and validation, and each observation is used for validation exactly once.

The fitting of various coefficients parameter in the equation (4) was done using all dataset (fitting errors are about 2 dB for all polarizations). This fitting allows writing σ° as a function of the rms surface height (*Hrms*) and incidence angle (θ), by equations (5), (6) and (7):

$$\sigma_{HH}^{\circ} = 10^{-1.287}(\cos\theta)^{1.227}\ 10^{0.009\, cotan(\theta)\, mv}\ (kHrms)^{0.86\, sin(\theta)}, \tag{5}$$

$$\sigma_{VV}^{\circ} = 10^{-1.138}(\cos\theta)^{1.528}\ 10^{0.008\, cotan(\theta)\, mv}\ (kHrms)^{0.71\, sin(\theta)} \tag{6}$$

$$\sigma_{HV}^{\circ} = 10^{-2.325}(\cos\theta)^{-0.01}\ 10^{0.011\, cotan(\theta)\, mv}\ (kHrms)^{0.44\, sin(\theta)}, \tag{7}$$

where θ is expressed in radians and *mv* is in vol.%. Equations (5), (6), and (7) show that the sensitivity (γ) of the radar signal to the soil moisture in decibel scale is 0.25 dB/vol.% in HH polarization, 0.22 dB/vol.% in VV polarization and 0.30 dB/vol.% in HV polarization for an incidence

angle of 20°. This sensitivity decreases to 0.09 dB/vol.% in HH, 0.08 dB/vol.% in VV and 0.11 dB/vol.% for an incidence angle of 45°. As for the signal's sensitivity to soil roughness, it is of the same order of magnitude in HH and VV and twice as large than that of the HV signal. The availability of a backscatter model for the cross polarization component is required because the most of spaceborne SAR acquisitions are made with one co-polarization and one cross-polarization in case of dual-polarization mode.

4.2. Results and discussion

4.2.1. Performance of the new model

Results show that the new model provides more accurate results. The biases and the RMSE decrease for both HH and VV polarizations. The RMSE decreases from 3.8 dB to 2.0 dB for HH and from 2.8 dB to 1.9 dB for VV (Table 3). In addition, the high over- or underestimations of radar backscattering coefficients observed with the Dubois model according to soil moisture, surface roughness and radar incidence angle are clearly eliminated with the new model (Figures 3 and 4).

Analysis of the new model's performance for each radar wavelength separately (L-, C- and X-bands) shows that the most significant improvement is observed in X-band with an RMSE that decreases from 4.1 dB to 1.9 dB in HH and from 3.2 dB to 1.8 dB in VV. In L-band, the performance of the new model is not better than that of the Dubois model because the RMSE decreases slightly with the new model of 3.0 dB to 2.3 dB in HH and remains similar in VV (RMSE = 2.3 dB with the Dubois model and 2.7 dB with the new model). The improvement is also important for the C-band with an RMSE that decreases from 3.7 dB to 1.9 dB in HH and from 2.6 dB to 1.9 dB in VV. With respect to bias, the results show that it decreases with the new model for all radar wavelengths. In addition, the new model does not show bias according the range of soil moisture, surface roughness, and radar incidence angle.

The comparison between the new model simulations in HV polarization (Equation 7) and the real data (SAR data) shows an RMSE of 2.1 dB (Table 3) (1.6 dB in L-band, 2.2 dB in C-band, and 1.9 dB in X-band). The bias (σ°SAR - model) is -1.3 dB in L-band, 0.2 dB in C-band, and -1.3 dB in X-band. Figure 5 shows also that the new model correctly simulates the radar backscatter coefficient in HV for all ranges of soil moisture, surface roughness and radar incidence angle.

Table 3. Comparison between the results obtained with the Dubois model and those obtained with the new model. Bias = real – model.

	Dubois for HH and VV		**New model**	
	Bias (dB)	**RMSE (dB)**	**Bias (dB)**	**RMSE (dB)**
HH for all data	-0.7	3.8	0.4	2.0
VV for all data	+0.9	2.8	0.0	1.9
HV for all data	-	-	0.0	2.1
HH, L-band	-0.8	2.9	-0.1	2.3
HH, C-band	-0.6	3.7	+0.3	1.9
HH, X-band	-0.7	4.1	0.7	1.9
VV, L-band	-0.2	2.3	-0.1	2.7
VV, C-band	+0.7	2.6	+0.1	1.9
VV, X-band	+2.0	3.2	-0.4	1.8
HV, L-band	-	-	-1.3	1.6
HV, C-band	-	-	+0.2	2.2
HV, X-band	-	-	-1.3	1.9

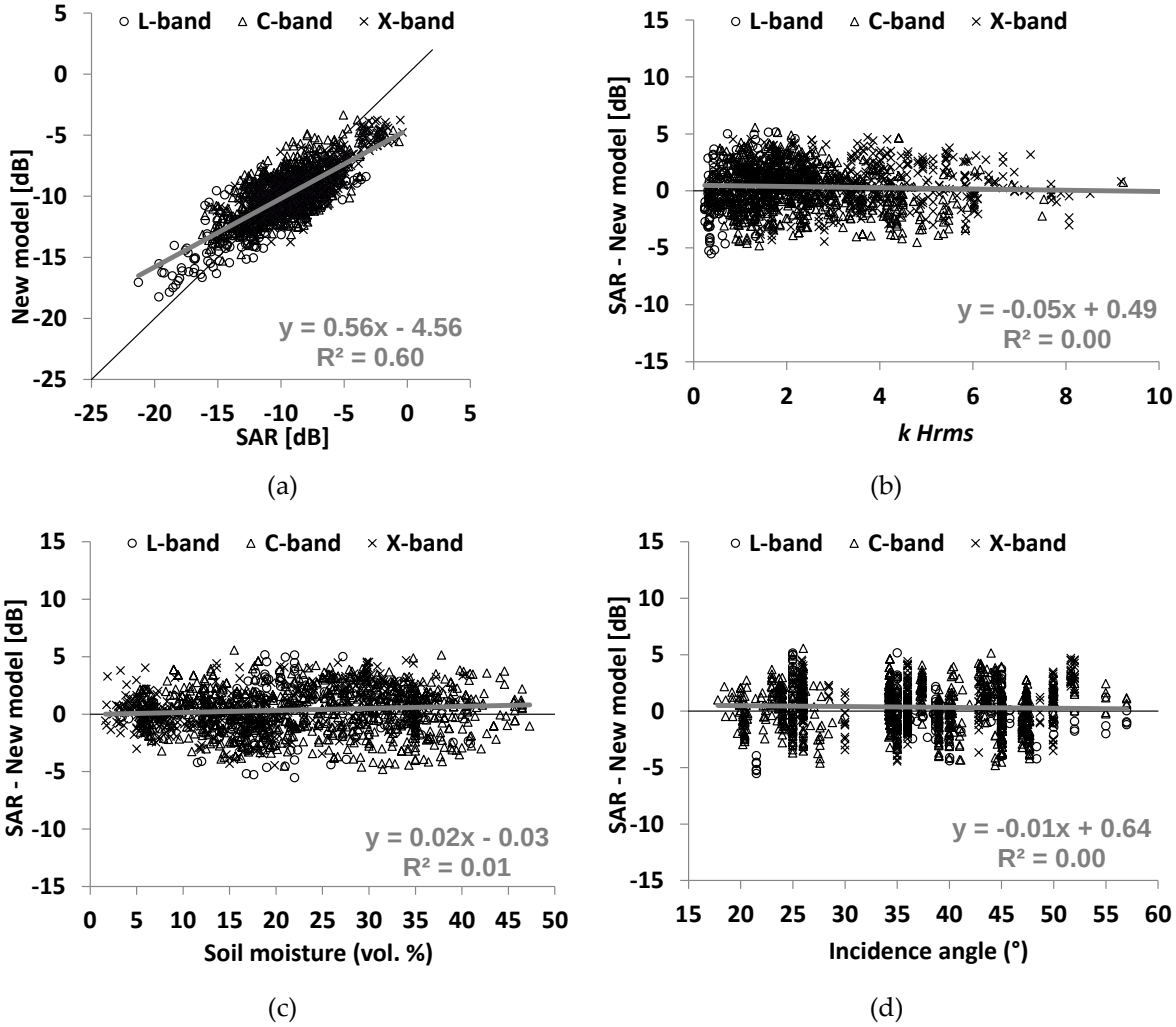

Figure 3. (a) Comparison between σ^{o} modelled in the new model and σ^{o} measured (for all SAR bands) for HH polarization, (b) difference between SAR and the new model as a function of surface roughness (*kHrms*), (c) difference between SAR and the new model as a function of soil moisture (*mv*), (d) difference between SAR and the new model as a function of incidence angle. The best regression model is ploted in gray.

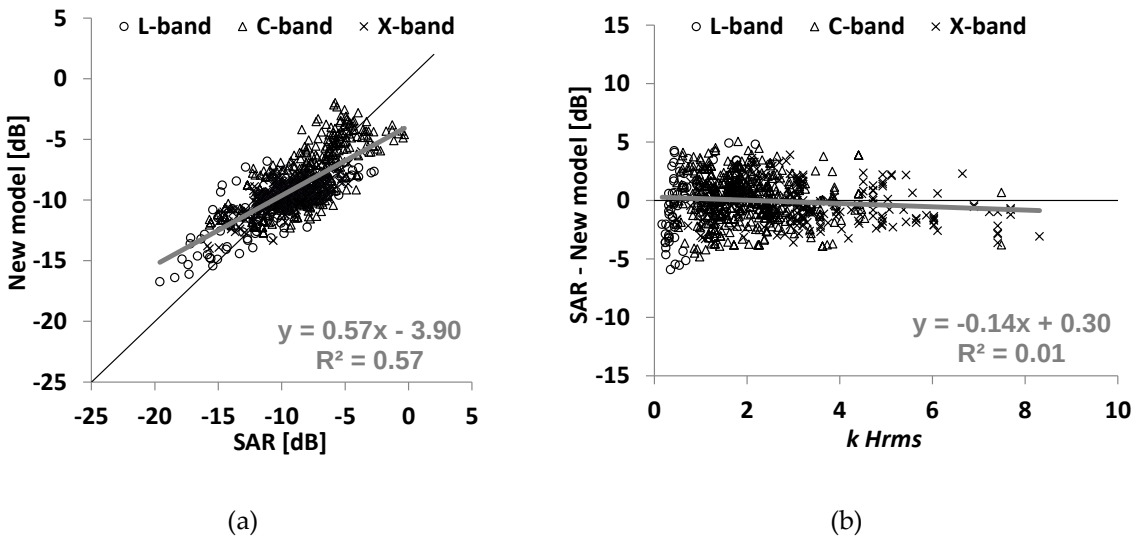

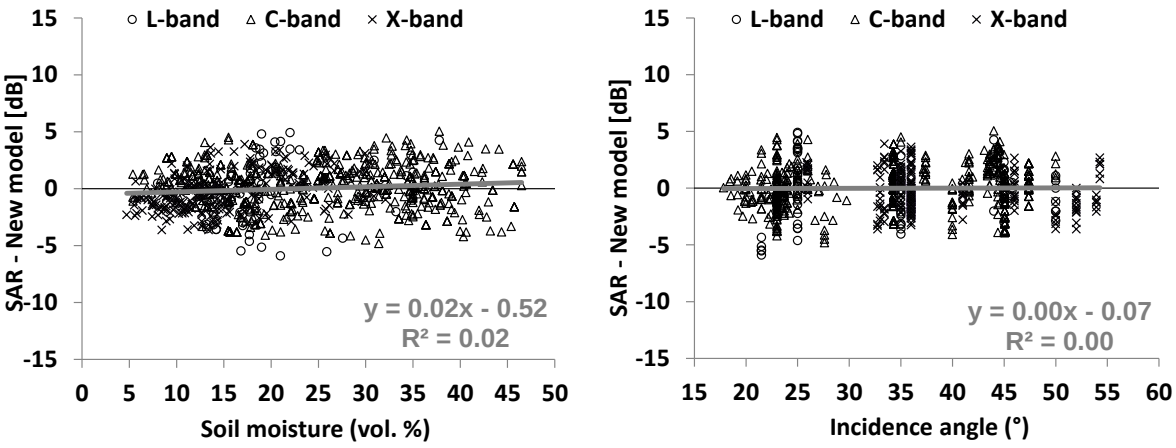

(c) (d)

Figure 4. (a) Comparison between σ^o in the new model and σ^o measured (for all SAR bands) for VV polarization, (b) difference between SAR and the new model as a function of surface roughness (*kHrms*), (c) difference between SAR and the new model as a function of soil moisture (*mv*), (d) difference between SAR and the new model as a function of incidence angle. The best regression model is ploted in gray.

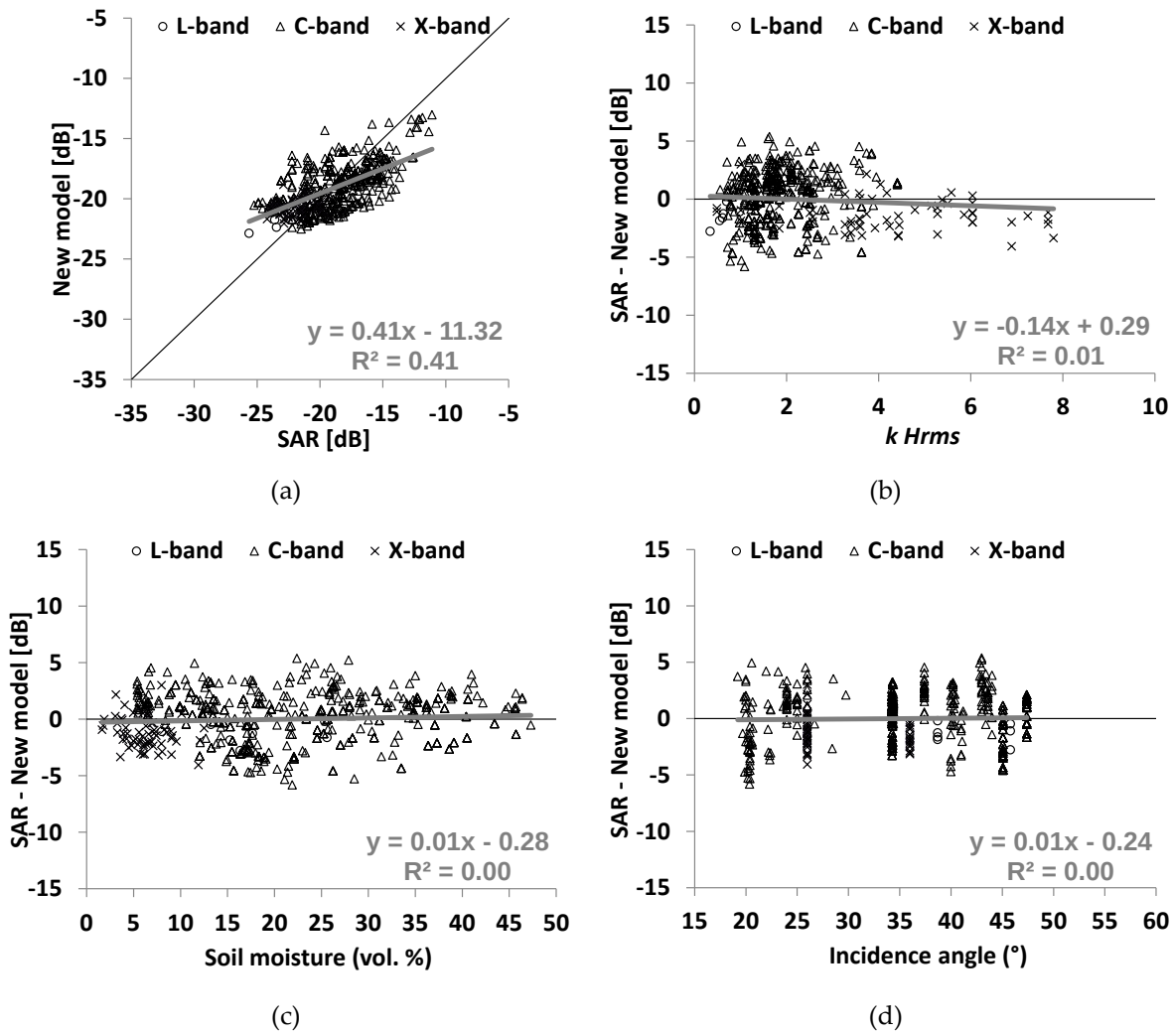

Figure 5. (a) Comparison between σ° in the new model and σ° measured (for all SAR bands) for HV polarization, (b) difference between SAR and the new model as a function of *kHrms*, (c) difference between SAR and the new model as a function of *mv*, (d) difference between SAR and the new model as a function of incidence angle. The best regression model is ploted in gray.

4.2.2. Behaviour of the new model

The physical behaviour of the new radar backscatter model was studied in function of incidence angle (θ), soil moisture (*mv*) and surface roughness (*kHrms*).

Figure 6 shows that the radar signal is strongly sensitive to surface roughness, especially for small values of *kHrms*. In addition, this sensitivity increases with the incidence angle. Concerning the influence of polarization, the new model shows, as do many theories and experimental studies, that a given soil roughness leads to slightly higher signal dynamics with the soil moisture in HH than in VV polarization [17,47]. The radar signal σ° increases with *kHrms*. This increase is higher for either low *kHrms* values or high θ-values than it is for either high *kHrms* values or low θ-values. For θ=45°, σ° increases approximately 8 dB in HH and 6.5 dB in VV when *kHrms* increases from 0.1 to 2 compared with only 3 dB when *kHrms* increases from 2 to 6 (for both HH and VV). This dynamic of σ° is only half for θ=25° in comparison to that for θ=45°. In HV, the dynamic of σ° to *kHrms* is half that observed for HH and VV.

The behaviour of σ° according to soil moisture shows a larger increase of σ° with *mv* for low incidence angles than for high incidence angles. Figure 6 shows that σ°_{HH} and σ°_{VV} increase approximately 6 dB for θ=25° compared with only 3 dB for θ=45° when *mv* increases from 5 to 35

vol.%. In HV, the signal increases approximately 7.5 dB for θ=25° and 3.5 dB for θ=45° when *mv* increases from 5 to 35 vol.%.

As mentioned in Dubois et al. [12], the ratio $\sigma^{\circ}_{HH}/\sigma^{\circ}_{VV}$ should increase with *kHrms* and remain less than 1. The new model shows that this condition is satisfied when 20°< θ <45°, *kHrms* < 6 and *mv* < 35 vol.%.

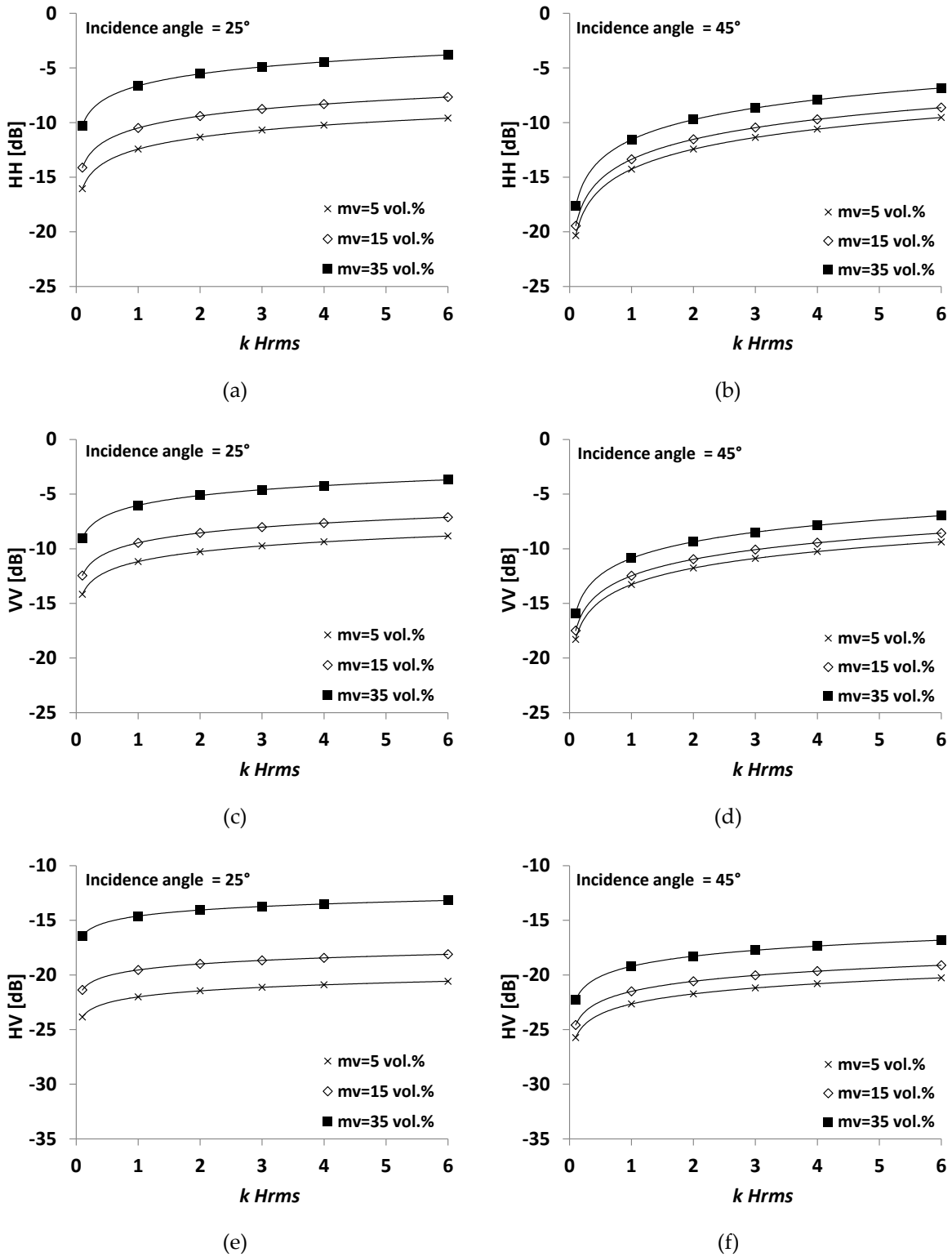

Figure 6. Behavior of the new model as a function of incidence angle, surface roughness (*k Hrms*) and soil moisture (*mv*) in HH, VV and HV polarizations.

5. Conclusion

This investigations objective is to propose a new empirical model for radar backscatter from bare soil surfaces. The new model is based on the formulation made in the Dubois model where the radar signal in HH and VV polarizations is described according to radar wavelength, incidence angle, soil moisture and roughness. This new model is based on the formulation made in the Dubois model. A large dataset was used, composed of ground measurements and SAR images over bare agricultural soils.

Results show that the new model provides improved results in comparison to the Dubois model (in the case of HH and VV). Biases and RMSE have decreased for both HH and VV polarizations. In addition, the high over- or under-estimations observed with the Dubois model for some ranges of soil moisture, surface roughness and radar incidence angle were clearly eliminated with the new model. Analysis of the new model's performance for each radar wavelength separately (L, C and X) shows that in the L-band, the performance of the new model was similar to that of the Dubois model. The model shows significant improvement in C- and X-bands (RMSE approximately 1.9 dB with the new model and between 2.6 and 4.1 dB with the Dubois model).

Based on the same equation as that used for HH and VV, a radar signal in HV polarization was also proposed. Finally, the new empirical model proposed in the present study would allows more accurate soil moisture estimates using the new Sentinel-1A and -1B SAR data.

Acknowledgements: This research was supported by IRSTEA (National Research Institute of Science and Technology for Environment and Agriculture), the French Space Study Center (CNES, TOSCA 2016) and the Belgian Science Policy Office (Contract SR/00/302). H. Lievens is a postdoctoral research fellow of the Research Foundation Flanders (FWO). Authors thank the space agencies that provided AIRSAR, SIR-C, JERS-1, ERS-1/2, RADARSAT-1/2, ASAR, PALSAR-1, TerraSAR-X, COSMO-SkyMed, and ESAR data.

References

1. Rao, S.S.; Kumar, S.D.; Das, S.N. Modified dubois model for estimating soil moisture with dual polarized SAR data. J. Indian Soc. Remote Sensing, 41, p. 865–872, 2013.
2. Chai, X.; Zhang, T.T.; Shao, Y.; Gong, H.Z.; Liu, L.; Xie, K.X. Modeling and mapping soil moisture of plateau pasture using RADARSAT-2 imagery. Remote Sensing, 7, p. 1279–1299, 2015.
3. Kirimi F., Kuria D.N., Frank Thonfeld F., Amler E., Mubea K., Misana S., Gunter Menz G., 2016. Influence of Vegetation Cover on the Oh Soil Moisture Retrieval Model: A Case Study of the Malinda Wetland, Tanzania. Advances in Remote Sensing, 5, p. 28-42, 2016.
4. Gherboudj I., Magagi R., Berg A.A., Toth B., Soil moisture retrieval over agricultural felds from multi-polarized and multi-angular RADARSAT-2 SAR data. Remote Sensing of Environment, 115, p. 33-43, 2011.
5. Zribi M., Chahbi A., Shabou M., Lili-Chabaane Z., Duchemin B., Baghdadi N., Amri R., Chehbouni A., Soil surface moisture estimation over a semi-arid region using ENVISAT ASAR radar data for soil evaporation evaluation. Hydrology and Earth System Sciences, 15, p. 345-358, 2011.
6. Le Hegarat-Mascle S., Zribi M., Alem F., Weisse A., Loumagne C., Soil moisture estimation from ERS/SAR data: Toward an operational methodology. IEEE Transactions on Geoscience and Remote Sensing 40/12, p. 2647-2658, 2002.
7. Zribi M., Dechambre M., A new empirical model to retrieve soil moisture and roughness from Radar Data. Remote Sensing of Environment, 84/1, p. 42-52, 2003.
8. Oh Y., Sarabandi K., Ulaby F.T., An empirical model and an inversion technique for radar scattering from bare soil surfaces . IEEE Transactions on Geoscience and Remote Sensing, 30(2), p. 370-381, 1992.

9. Oh Y., Kay Y., Condition for precise measurement of soil surface roughness. IEEE Transactions on Geoscience and Remote Sensing, 36(2), p. 691-695, 1998.
10. Oh Y., Sarabandi K., Ulaby F.T., Semi-empirical model of the ensemble-averaged differential Mueller matrix for microwave backscattering from bare soil surfaces. IEEE Transactions on Geoscience and Remote Sensing, 40, p. 1348-1355, 2002.
11. Oh Y., Quantitative retrieval of soil moisture content and surface roughness from multipolarized radar observations of bare soil surfaces. IEEE Transactions on Geoscience and Remote Sensing, 42, p. 596-601, 2004.
12. Dubois P.C., Van Zyl J., Engman T., Measuring soil moisture with imaging radars. IEEE Transactions on Geoscience and Remote Sensing, 33, p. 915-926, 1995.
13. Baghdadi N., Saba E., Aubert M., Zribi, M., Baup F., Comparison between backscattered TerraSAR signals and simulations from the radar backscattering models IEM, Oh, and Dubois. IEEE Geosci. Remote Sens. Lett. 8, p. 1160–1164, 2011.
14. Baghdadi N., Zribi M., Evaluation of radar backscatter models IEM, Oh and Dubois using experimental observations. Int. J. Remote Sens., 27, p. 3831–3852, 2006.
15. Wang H., Méric S., Allain S., and Pottier E., Adaptation of Oh Model for Soil Parameters Retrieval Using Multi-Angular RADARSAT-2 Datasets. Journal of Surveying and Mapping Engineering, 2(4), p. 65-74, 2014.
16. Wang J.R., Hsu A., Shi J.C., O'Neill P.E., Engman E.T., A comparison of soil moisture retrieval models using SIR-C measurements over the Little Washita River watershed». Remote Sensing Environment, 59, p. 308–320, 1997.
17. Zribi M., Taconet O., Le Hégarat-Mascle S., Vidal-Madjar D., Emblanch C., Loumagne C., Normand M., Backscattering behavior and simulation comparison over bare soils using SIRC/XSAR and ERASME 1994 data over Orgeval. Remote Sensing of Environment, 59(2), p. 256-266, 1997.
18. Baghdadi N., Dubois-Fernandez P., Dupuis X., Zribi M., Sensitivity of mail polarimetric parameters of multifrequency polarimetric SAR data to soil moisture and surface roughness over bare agricultural soils. IEEE Geoscience and Remote Sensing Letters, 10(4), p. 731-735, 2013.
19. Baghdadi N., Zribi M., Loumagne C., Ansart P., Paris Anguela T., Analysis of TerraSAR-X data and their sensitivity to soil surface parameters over bare agricultural fields. Remote Sensing of Environment, 112(12), p. 4370-4379, 2008.
20. Baghdadi N., Aubert M., Zribi M., Use of TerraSAR-X data to retrieve soil moisture over bare soil agricultural fields. IEEE Geoscience and Remote Sensing Letters, 9(3), p. 512-516, 2012.
21. Baghdadi N., Gherboudj I., Zribi M., Sahebi M., Bonn F., King C., Semi-empirical calibration of the IEM backscattering model using radar images and moisture and roughness field measurements. International Journal of Remote Sensing, 25(18), p. 3593-3623, 2004.
22. Baghdadi N., King C., Bourguignon A., Remond A., Potential of ERS and RADARSAT data for surface roughness monitoring over bare agricultural fields : application to catchments in Northern France. International Journal of Remote Sensing, 23(17), p. 3427-3442, 2002.
23. Holah H., Baghdadi N., Zribi M., Bruand A., King C., Potential of ASAR/ENVISAT for the characterisation of soil surface parameters over bare agricultural fields. Remote Sensing of Environment, 96(1), p. 78-86, 2005.
24. Baghdadi N., Holah N., Zribi M., Calibration of the Integral Equation Model for SAR data in C-band and HH and VV polarizations. International Journal of Remote Sensing, 27(4), p. 805-816, 2006.
25. Le Morvan A., Zribi M., Baghdadi N., and Chanzy A., Soil moisture profile effect on radar signal measurement. Remote Sensing, 8, p. 256-270, 2008.
26. Baghdadi N., Saba E., Aubert M., Zribi M., Baup F., Comparison between backscattered TerraSAR signals and simulations from the radar backscattering models IEM, Oh, and Dubois, IEEE Geoscience and Remote Sensing Letters, 8(6), p.1160-1164, doi: 10.1109/LGRS.2011.2158982, 2011.

27. Baghdadi N., Cresson R., El Hajj M., Ludwig R., La Jeunesse I., Estimation of soil parameters over bare agriculture areas from C-band polarimetric SAR data using neural networks. Hydrology and Earth System Sciences (HESS), 16, p. 1607-1621, doi:10.5194/hess-16-1607-2012, 2012.
28. Baghdadi N., Aubert M., Cerdan O., Franchistéguy L., Viel C., Martin E., Zribi M., Desprats J.F., Operational mapping of soil moisture using synthetic aperture radar data: application to Touch basin (France). Sensors Journal, 7, p. 2458-2483, 2007.
29. Zribi M., Gorrab A., Baghdadi N., Lili-Chabaane Z., Influence of radar frequency on the relationship between bare surface soil moisture vertical profile and radar backscatter, IEEE Geoscience and Remote Sensing Letters, 11(4), p. 848-852, doi: 10.1109/LGRS.2013.2279893, 2014.
30. Gorrab A., Zribi M., Baghdadi N., Mougenot B., Lili-Chabaane Z., Retrieval of both soil moisture and texture using TerraSAR-X images, Remote Sensing, 7, p. 10098-10116, doi:10.3390/rs70810098, 2015.
31. Aubert M., Baghdadi N., Zribi M., Ose K., El Hajj M., Vaudour E., Gonzalez-Sosa E., Toward an operational bare soil moisture mapping using TerraSAR-X data acquired over agricultural areas, IEEE Journal of Selected Topics in Applied Earth Observations and Remote Sensing (JSTARS), 6(2), p. 900-916, doi: 10.1109/JSTARS.2012.2220124, 2013.
32. Dong L., Baghdadi N., Ludwig R., Retrieving surface soil moisture using radar imagery in a semi-arid environment. IEEE Geoscience and Remote Sensing Letters, 10(3), p. 461-465, 2013.
33. Baup F., Fieuzal R., Marais-Sicre C., Dejoux J-F., le Dantec V., Mordelet P., Claverie M., Hagolle O., Lopes A., Keravec P., Ceschia E., Mialon A., Kidd R., MCM'10: An experiment for satellite multi-sensors crop monitoring. From high to low resolution observations, Geoscience and Remote Sensing Symposium, p. 4849-4852, 2012.
34. Mattia M., Toan T.L., Souyris J.C., Carolis G.D., Floury N., Posa F., Pasquariello G., The effect of surface roughness on multifrequency polarimetric SAR data. IEEE Trans. Geosci. Remote Sens., 35(4), p. 954–966, 1997.
35. Lievens H., Verhoest N.E.C., De Keyser E., Vernieuwe H., Matgen P., Álvarez-Mozos J., De Baets B., Effective roughness modelling as a tool for soil moisture retrieval from C-and L-band SAR, Hydrology and Earth System Sciences, 15(1), p. 151-162, 2011.
36. Baronti S., Del Frate F., Ferrazzoli P., Paloscia S., Pampaloni P., Schiavon G., SAR polarimetric features of agricultural areas, International Journal of Remote Sensing, 16(14), p. 2639-2656, 1995.
37. Macelloni G., Paloscia S., Pampaloni P., Sigismondi S., de Matthæis P., Ferrazzoli P., Schiavon G., Solimini D., The SIR-C/X-SAR experiment on Montespertoli: sensitivity to hydrological parameters, International Journal of Remote Sensing, 1999, 20(13), p. 2597-2612, 1999.
38. Paloscia S., Macelloni G., Pampaloni P., Sigismondi S., The potential of C- and L-band SAR in estimating vegetation biomass: the ERS-1 and JERS-1 Experiments, IEEE Trans.on Geosci. and Remote Sensing, 37(3), p. 2107-2110, 1999.
39. Ulaby F.T., Moore R.K., Fung A.K., Microwave Remote Sensing, vol. II (New York: Addison-Wesley), 1982.
40. Beauchemin M., Thomson K., Edwards G., Modelling forest stands with MIMICS: implications for calibration. Canadian Journal of Remote Sensing, 21, p. 518–526, 1995.
41. Baghdadi N., Bernier M., Gauthier R., Neeson I., Evaluation of C-band SAR data for wetlands mapping. International Journal of Remote Sensing, 22, p. 71–88, 2001.
42. Baghdadi N., Holah N., Zribi M., Soil moisture estimation using multi-incidence and multi-polarization ASAR SAR data. In: International Journal of Remote sensing, 27/10, p. 1907-1920, 2006.
43. Aubert M., Baghdadi N., Zribi M., Douaoui A., Loumagne C., Baup F., El Hajj M., Garrigues S., Characterization of soil surface by TerraSAR-X imagery. Remote Sensing of Environment, 115, p. 1801–1810, 2011.

44. Baghdadi N., Cerdan O., Zribi M., Auzet V., Darboux F., El Hajj M., Bou Kheir R., Operational performance of current synthetic aperture radar sensors in mapping soil surface characteristics in agricultural environments: application to hydrological and erosion modelling. Hydrological Processes, 22, p. 9-20, 2008.
45. Srivastava H.S., Patel P., Manchanda M.L., Adiga S., Use of multi-incidence angle RADARSAT-1 SAR data to incorporate the effects of surface roughness in soil moisture estimation. IEEE Transactions on Geosciences and Remote Sensing, 41, p. 1638-1640, 2003.
46. Sahebi M.R., Angles J., Bonn F., A comparison of multi-polarization and multi-angular approaches for estimating bare soil surface roughness from spaceborne radar data. Canadian Journal of Remote Sensing, 28(5), p. 641-652, 2002.
47. Fung A. K., 1994. Microwave Scattering and Emission Models and their Applications. Artech House, Inc., Boston, London, 573 pages.

© 2016 by the authors. Submitted for possible open access publication under the terms and conditions of the Creative Commons Attribution (CC-BY) license (http://creativecommons.org/licenses/by/4.0/).